VALIDATION OF A MULTI-ZONE MODEL WITH INTEGRATED ENERGY EQUATION AND IMPACT OF THERMAL MASS MODELING METHODOLOGY

Jinchao Yuan and Leon R. Glicksman
Building Technology Program
Massachusetts Institute of Technology
5-418, 77 Massachusetts Ave, Cambridge, MA 02139

ABSTRACT

In this paper, the issue of thermal mass modeling is investigated in the process of validating an integrated multi-zone program that couples energy equation solving for air and thermal mass temperatures.

The predicted air temperatures in different spaces are preliminarily compared with the field measurement data to validate the program. The discrepancies are analyzed and explained by the direct radiation absorption of the thermal mass. Sensitivity analysis of the radiation absorption ratio on the air and thermal mass temperature predictions are conducted.

The validation is conducted again based on the sensitivity analysis. A simple radiation module is developed to estimate the portion of direct radiation to the thermal mass. The agreement between simulation and measurement data shows overall improvements with proper consideration of the radiation absorption.

INTRODUCTION

Multi-zone models are fast and simple models to predict bulk flows within the buildings. In a multi-zone model, the spaces are modeled as nodes and the openings such as doors and windows are modeled as branches. In a general multi-zone model, the pressures of these nodes and the airflows through these paths are solved. Although it is a general practice to couple multi-zone airflow models such as CONTAMW and COMIS into Energy/Plant simulation programs such as EnergyPlus (EnergyPlus™ 2004), ESP-r (Beausoleil-Morrison, 2000), and TRNSYS (McDowell et. al, 2003), most of the stand alone multi-zone programs do not incorporate energy equations to solve temperatures due to the additional complexities involved in describing and solving the problem. Axley (2001) developed a modified version of CONTAMW (internally named CONTAMR97) that coupled heat transfer solving into the multi-zone model and applied it into natural ventilation design studies. However, the program has not been in publicity due to occasional numerical problems reported by the author (Axley et. al, 2002).

For natural ventilation, especially buoyancy driven flows, the temperature solving becomes crucial because the temperature differences between zones are the dominant driven forces of the flows. To model natural ventilation flows, an integrated transient multi-zone simulation program is developed for design simulations based on a prototype steady state multi-zone model developed by Tan (2005). The program is simplified for dealing with issues such as large openings, wind pressure coefficient, and temperature solving, which are key factors in natural ventilation. Mechanical systems such as Air Handling Units and duct systems are not considered as is in other

programs such as CONTAMW (Dols and Walton, 2002). It allows less technologically sophisticated users to quickly select and compare different natural ventilation design strategies.

The program solves transient airflows, air temperatures, and thermal mass temperatures simultaneously. Figure 1 shows the three integrated modules of the program: the airflow module, the air temperature module, and the thermal mass module.

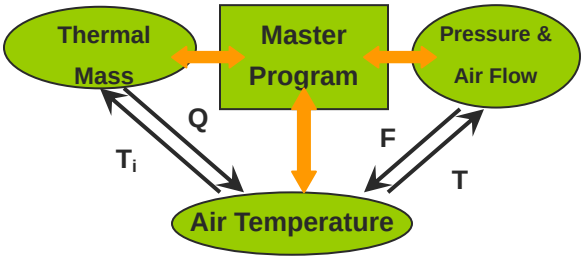

Figure 1. An integrated airflow, heat transfer, and thermal mass solving program

The governing equations for the airflow module are the mass balance and flow path pressure relationship equations similar to other multi-zone programs such as CONTAMW (Dols and Walton, 2002).

The air temperature module solves the first order air temperature dynamics in the following way:

$$\rho V c_p \frac{dT_i}{dt} = -\sum_j f_{ij} \rho c_p T_i + \sum_j f_{ji} \rho c_p T_j + S_i + hA(T_{m1} - T_i) \quad (1)$$

where T_{m1} is temperature of the first layer of the connected thermal mass. h is the convective heat transfer coefficient between the air and the thermal mass and A is the contact area between them. The term $hA(T_{m1}-T_i)$ accounts for the rate of convective heat transfer from the thermal mass to the air.

The thermal mass module discretizes the thermal mass into thin layers with a criterion of Biot Number $Bi < 0.2$, which defined by:

$$Bi = hL/k \quad (2)$$

where h is the surface convective heat transfer coefficient, L is the thickness of the layer, and k is the conductivity of the slab. Only one-dimensional heat transfer through the thickness direction is considered. Figure 2 shows the configuration of this simulation method. The boundary conditions of this module are determined by the air temperature (T_i, T_k) and rate of direct radiation (Q_{b1}, Q_{b2}) absorption, and the thermal mass configuration. Given a set of boundary conditions, the linear network can be quickly solved by standard circuit network analogies.

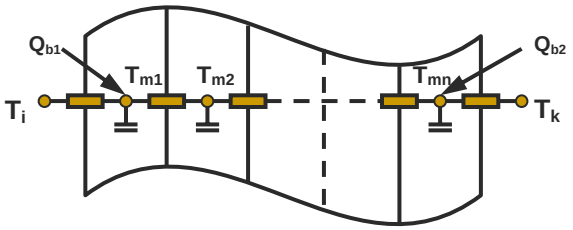

Figure 2. The thermal mass simulation methodology

The air flow module, the air temperature module, and the thermal mass temperature model are coupled and exchange information during each time step of simulation. Since the thermal mass temperature changes much slower than the air temperature, the air temperature module will use the T_{m1} of the previous step to calculate the new air temperature T_i and Q_{b1}. The newly calculated T_i and Q_{b1} will be used as boundary conditions for the thermal mass module to calculate the new thermal mass temperatures.

VALIDATION

To validate the integrated model, the transient simulation results are compared with the field measurement data collected in August 2003, when the on-site temperatures of a naturally ventilated building are logged at an interval of 15 minutes for a month in a previous study by Walker et. al (2004).

Figure 3 shows the naturally ventilated building to be investigated. It is a three-floor building located in Luton, United Kingdom, with a dimension of 25m×17.2m×14.5m. The actual orientation of the building is Northeast-Southwest. In the present study, we simply denote the Northeast side as North side and the Southwest side as South side. The building consists of an atrium space in the middle and multiple office spaces on the two sides.

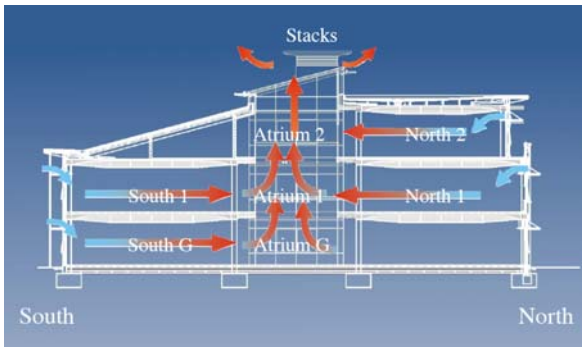

Figure 3. The natural ventilation system of Houghton Hall (Spindler, 2004)

Figure 4 shows the configuration of one of the office spaces on the north side. The north wall (for the south side office, south wall) of the office is 45% glazed. Seven windows are aligned on the same side. Each window has an upper vent which is open all the time from April to October and a lower awning part which is open during work hours in weekdays. The other side of the office space is open to the central atrium area. The space has a carpeted and raised floor. The ceiling is an exposed concrete slab with a thickness of 10cm. Further, the office is usually occupied by 12-15 persons in general and each has a computer.

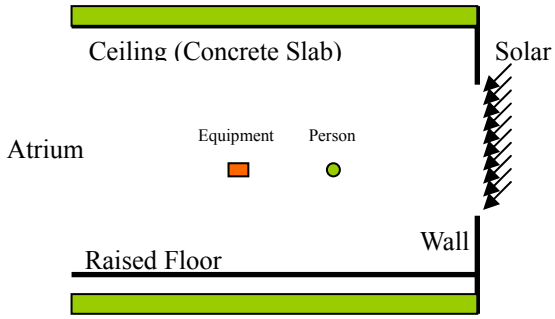

Figure 4. The illustration of one north office

Solar radiation through the windows, the most important heat source, is calculated by the method illustrated by Duffie and Beckman (1991). The method takes the horizontal solar radiation (from measurement), time (month, hour, minute), and window orientation as input. The direct, diffuse, and reflective (by the ground) components of the solar radiation in the direction normal to the window are decomposed from horizontal radiation and the total incoming solar radiation is the sum of the three.

Other boundary conditions such as such as outdoor air temperature, wind velocity, and internal load profile during the monitoring period can be obtained from field measurement or the National Renewable Energy Lab (NREL, http://www.nrel.gov/) weather file. Based on the available information, the entire building was simulated by the developed program for a period of two weeks from mid to late August 2003.

PRELIMINARY RESULTS

Figure 5a and 5b shows the simulation results by assuming no radiation absorption by the thermal mass. Namely, the solar heat gain is lumped with internal loads and is injected into the space air mainly by convection. The results are compared

with the field measurement data collected by Walker et. al (2004). Figure 4a shows that the simulation results have a larger swing than the actual monitoring data. Similar pattern happens in the North space on the second floor (see Figure 5b). The actual measured data also show a lag behind the simulation results. Although there are numerous causes for the discrepancies between prediction and field measurement, this implies the thermal mass effect may have a stronger effect than the model has suggested.

For a steady state simulation, it can be assumed that the solar radiation is lumped with internal loads. In other words, the heat load is assumed to go directly to the space air. However, for transient simulations, especially for solar heat gains, part of the heat source is directly injected to the thermal mass surface by radiation and is partly absorbed there. Typical examples of this effect are the solar radiation and internal low temperature radiation to the floor, wall, or ceiling. Therefore the distribution of the heat load becomes important for transient simulations and the internal radiation should be adequately considered.

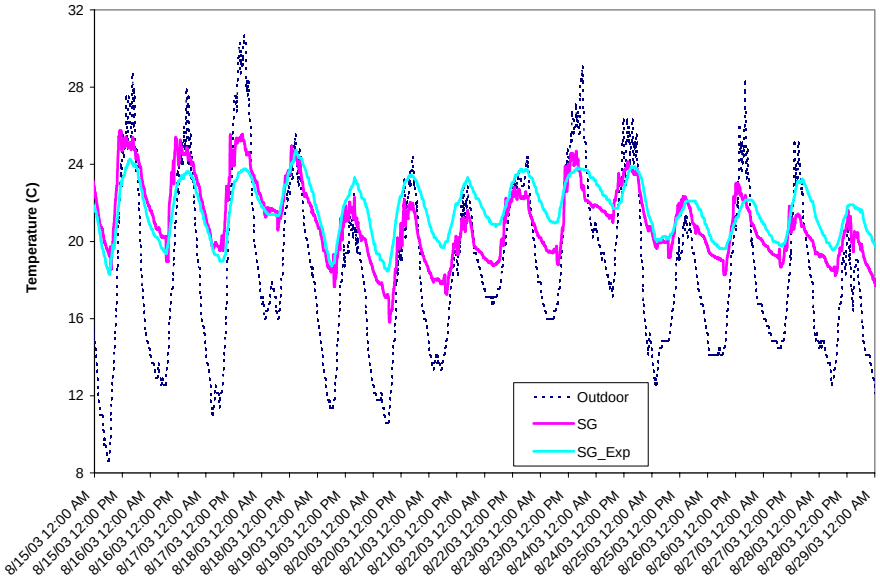

(a)

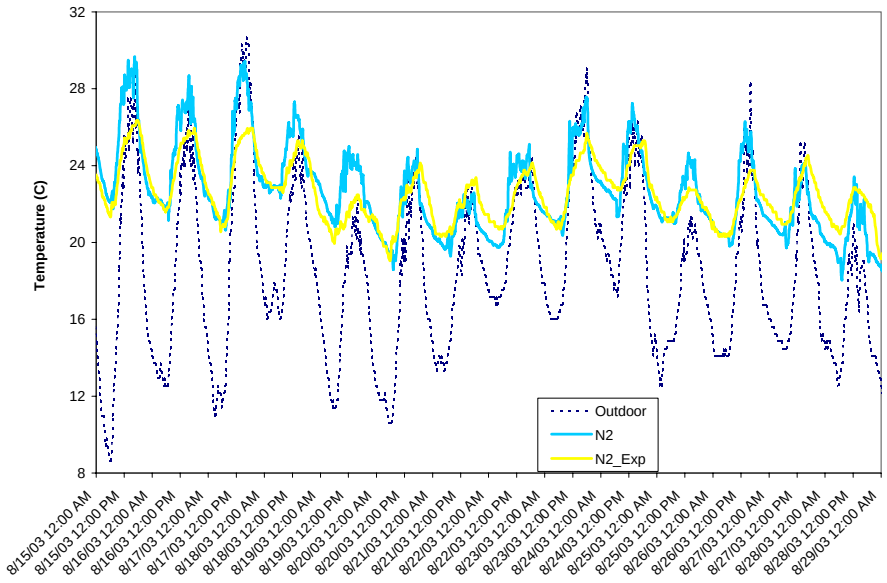

(b)

Figure 5. Comparison between simulation and field measurements in (a) South office on the ground floor (b) North office on the 2nd floor

ANALYSIS

Previous studies in the internal radiation and the heat source distribution models (see EnergyPlus™ 2004) generally applies detailed surface energy balanced equations and calculates view factors between surfaces. Although building such a model is not the immediate goal of the present study, the internal radiation effects can be investigated by our integrated program. Figure 6 shows the way that the heat load distribution affects the model by examining a zone with a thermal mass slab. The temperature in zone i is denoted as T_i. The space load, including both internal and solar, is denoted as S_i. For simplicity, the thermal mass is assumed to be the only thermal mass in this zone.

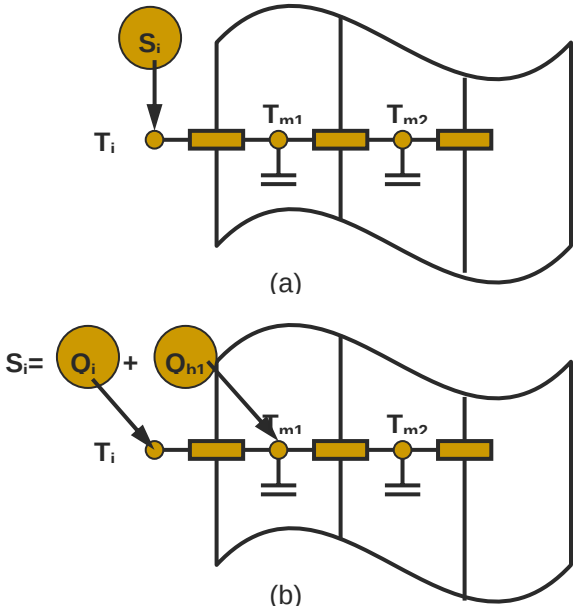

Figure 6. Model mechanism: (a) heat load

lumped as internal (b) heat load distributed as internal and direct absorption

Figure 6a demonstrates the model configuration if the space heat load only transfers to the air (mainly by convection or conduction). The only way for the first layer of the thermal mass (with temperature T_{m1} in the figure) to exchange heat with the air is by surface convection. In this scenario, equation 1 is exactly the dynamical system equation for the air temperature T_i in zone i. Figure 6b shows how the system modeling methodology changes when part of the total load (Q_{b1}) goes to the wall surface (by radiation) and gets absorbed there. The total load (S_i) is kept the same as that in the first scenario. In this new scenario, the term S_i in equation 1 should be replaced by Q_i. If we define a fraction of the heat absorbed by the thermal mass as $\alpha = Q_{b1}/S_i$, equation 1 will become the following:

$$\rho V c_p \frac{dT_i}{dt} = -\sum_j f_{ij}\rho c_p T_i + \sum_j f_{ji}\rho c_p T_j + (1-\alpha)S_i + hA(T_{m1} - T_i) \quad (3)$$

On the thermal mass circuit network side, there is also a change to be made when there is direct absorption. It is handled as an additional current source Q_{b1} (or αS_i) connected on the first node T_{m1} of the circuit network (see Figure 6b).

Figure 6b also provides a general framework on how to integrate our program with a more complicated internal radiation model. As far as the distribution that is determined by α can be calculated on a specific internal radiation model, the internal radiation module can be plugged into the program to calculate the radiation effect.

A sensitivity study is conducted for results shown in Figure 4a but with different α values (for Figure 4a, α=0). The results are plotted on Figure 7. The series of curves show that when thermal mass absorption increases its ratio, the predicted space air temperature varies in smaller amplitude due to the damping effect of thermal mass. The differences of the air temperature for different α values can reach ~2 ºC in peak load periods.

In reality, the actual α value is changing all the time with different combinations of the surface temperature, air temperature, and heat source strength. Internal radiance models are needed to calculate the thermal mass surface temperatures and solve the heat transfers between the thermal mass, the heat sources, and the façade system. Through results obtained in these detailed models, α can be simultaneously found in the run and provide the program with more accuracy.

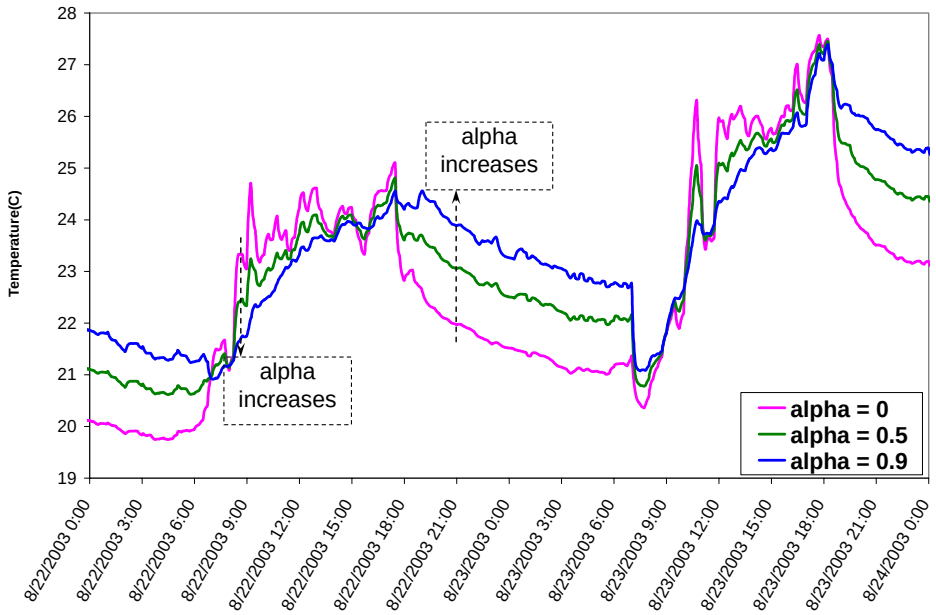

Figure 7. Predicted air temperature for three different α values in North Second Floor office

REVISIT

Since α alpha value is an important factor in modeling the airflow and heat transfer of the system, it is important to consider it properly in a simulation. A simple internal radiation model is considered to estimated the α value.

Figure 8 shows the simple radiation model corresponding to the office space shown in Figure 4. Since the office has a carpeted raised floor, it has a large thermal resistance for vertical heat transfer beneath the raised floor surface. Therefore, the floor downside is assumed to be adiabatic in this simplified model. The shortwave solar radiation and long wave (infrared) radiation are considered. The solar radiation coming from the window is assumed to inject to the floor first and then be absorbed / reflected. All surfaces are assumed to be diffusive gray surfaces.

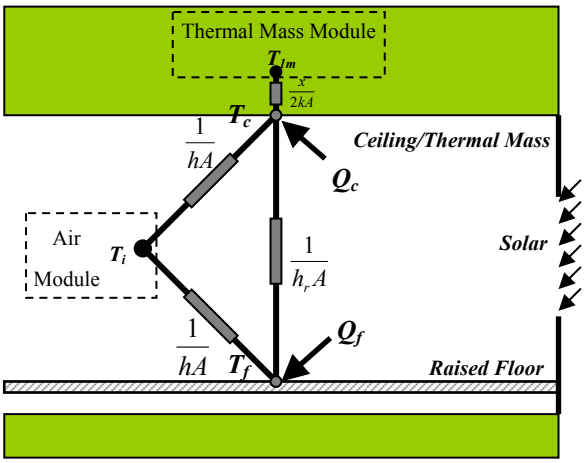

Figure 8. Internal Radiation model

Two surface heat balance equations are to be solved for the ceiling surface temperature T_c and the floor surface temperature T_f.

$$(T_{1m} - T_c) \cdot 2kA / x + Q_c + (T_i - T_c) \cdot hA + (T_f - T_c) \cdot h_r A = 0 \quad (4)$$

and

$$Q_f + (T_i - T_f) \cdot hA + (T_c - T_f) \cdot h_r A = 0 \quad (5)$$

where h_r is the effective thermal resistant between the ceiling and the floor surfaces through radiation.

The emissions and reflections from the wall surface to the ceiling / floor is not considered in this estimation since the view factor from the floor to ceiling dominates other view factors. Q_c is the radiative solar and internal heat grain transferred to the ceiling surface. Q_f is radiative solar and internal heat gain transferred to the floor surface.

The incoming solar is absorbed and reflected multiple times inside the space before gaining an equilibrium distribution. Since the absorptance for the solar is in the range of 0.65 - 0.80 (ASHRAE 2001), the solar is almost completely absorbed after two incidences. Therefore only one reflection was considered. The infrared radiation is also estimated. The guideline used in internal load calculation by ASHRAE (2001) was applied to split the convective and radiation. A split of 50% convective, 50% radiative was recommended for equipment, while a split of 40% convective, 60% radiative was recommended for occupant sensitive heat. Similarly to solar consideration, only first bounce is considered. Since the internal gain is much smaller than the solar gain in general, for simplicity, the radiation to the walls and windows is also neglected and thus an equal distribution between the ceiling and the floor is assumed. With these approximations, the term Q_c and Q_f used in equation (4) and (5) can be approximated as:

$$Q_c \approx \gamma_s(1-\gamma)S_{sol} \cdot X_{fc} + \gamma_i(0.5S_{equ} + 0.6S_{occ})/2 \quad (6)$$

$$Q_f \approx \gamma_s S_{sol} + \gamma_i(0.5S_{equ} + 0.6S_{occ})/2 \quad (7)$$

where γ_s is the absoprtance of the floor/ceiling surfaces for solar radiation and γ_i is for infrared raditon. X_{fc} is the view factor from the floor to the ceiling, which is about 0.75 in this configuration.

At each time step, when the internal zone temperature T_i obtained is first solved in the airflow and thermal network. The sub network in Figure 8 will be solved for the ceiling surface temperature T_c and floor surface temperature T_f. The α value can be approximately implied from the model by:

$$\alpha = \frac{Q_c + (T_f - T_c) \cdot h_r A}{S_{sol} + S_{equ} + S_{occ}} \quad (8)$$

The implied α value is changing with time and other conditions. It varies from 0 to 1, with an average value of 0.48 in this simulation.

Following the above analysis, the validation is rerun with the radiation model. The result shows improvements in the predictions in the South Ground office and North 2nd floor office compared to the field measurements. Figure 9 shows the simulation results in these two zones.

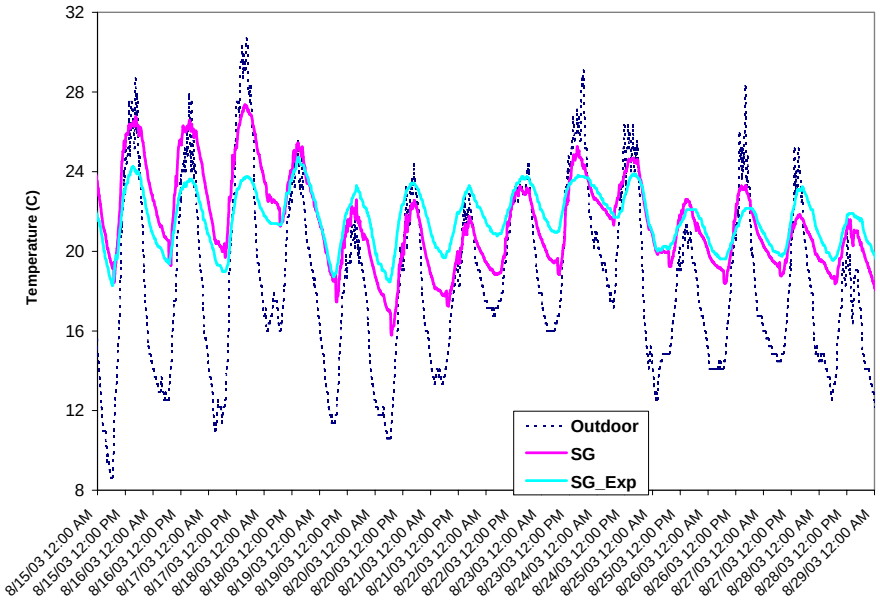

(a)

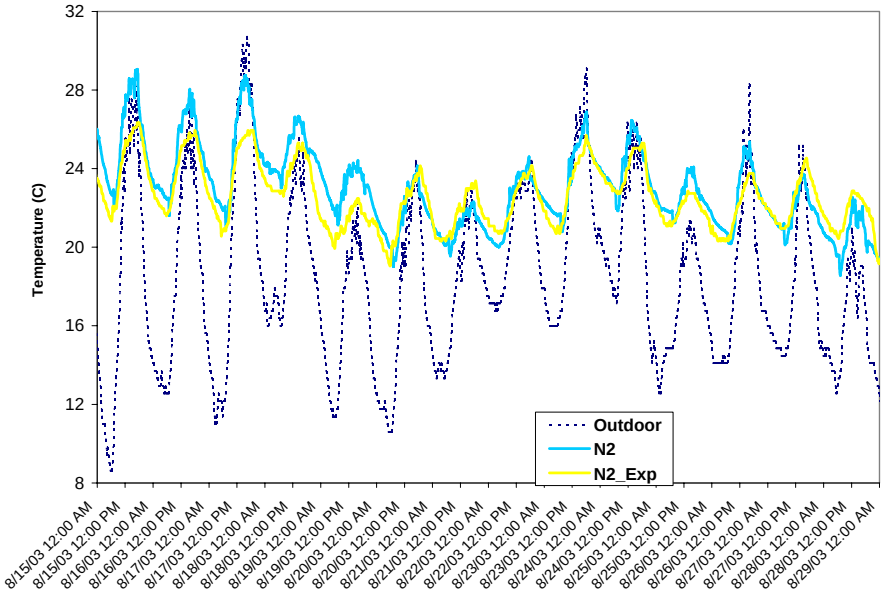

(b)

Figure 9. Comparison between simulation and field measurements in the (a) South office on the ground floor; (b) North office on the 2nd floor, both with radiation model

The results in Figure 9 show that the agreement between the program predictions and the field measurements has been improved compared to those in Figure 5 after Aug 18th. The improvement

is in two aspects. First, lead of the predicted result (in response to outdoor air temperature, heat load variation) to the measured data is reduced compared to the lead in Figure 5. Second, quantitatively, for the South office, the mean error is reduced from the original -0.67 °C to -0.21 °C with the radiation model. For the North 2nd office, the mean error is reduced from 0.52 °C to 0.23 °C.

The discrepancy between predicted and measured data in Figure 9 (Aug 15 to Aug 18) seems to be larger than that in Figure 5. However, this period is actually in an initial thermal mass "warming up" period (also described by Mehta, 2005) the simulation starts from a preset initial thermal mass temperature.

For the simulation in general, for both zones, the differences between the predictions and measurements are within ±1 °C for most of the time period. Other potential uncertainties are: 1). In hot days when the outdoor air temperature was relative high, fewer windows were opened by the occupants during the day. 2). The heating system could be turned on at night in actual building operations when the outdoor air temperatures dropped too low (usually <15 ºC). To further explain these discrepancies, more information on the building operations during the measurement period needs to be discovered and understood.

CONCLUSION

An integrated multi-zone program that can solve the air and thermal mass temperatures was developed for natural ventilation modeling. An actual natural ventilated building was selected to validate the accuracy of the program.

In the preliminary simulation, the model showed an under predicted pattern due to the assumption of the heat load distribution. The discrepancy was partly explained by the radiation absorbed by the thermal mass. A framework was developed to account for the absorption effect in a quantitative way and the thermal mass absorption ratio α is defined. A sensitivity test of the α value on the air temperature predictions was conducted to further demonstrate its impact. A revisit was conducted by estimating the portion of the radiation distribution using a simple radiation model for this case and the results showed overall improvements.

REFERENCE

ASHRAE, 2001. "ASHRE Handbook – Fundamentals," ASHREAE 2001, Atlanta, GA.

Axley, J.W, 2001. "Application of Natural Ventilation for U.S. Commercial Buildings; Climate Suitability, Design Strategies & Methods, Modeling Studies," GCR XXXX Draft report, 2001.

Axley, J., Emmerich, S., Dols, S., Walton, G., 2002. "An Approach to the Design of Natural and Hybrid Ventilation System for Cooling Buildings," *Proceedings of Indoor Air* 2002.

Beausoleil-Morrison, I., 2000, "The Adaptive Coupling of Heat and Air Flow Modeling Within Dynamic Whole-Building Simulation," Ph.D. Thesis, University of Strathclyde.

Duffie, J. A. and W. A. Beckman (1991). Solar Engineering of Thermal Processes. New York, John Wiley & Sons, Inc.

EnergyPlus™, 2004. "EnergyPlus Engineering Document: the Reference to EnergyPlus Calculations," the United States Department of Energy.

Spindler, H.C., 2004. “System Identification and Optimal Control for Mixed-Mode Cooling,” PhD Thesis. Massachusetts Institute of Technology.

Dols, W.S and Walton, G.N., 2002. “CONTAMW2.0 User Manual,” NISTIR 6921.

Tan, G., 2005. “Study of natural ventilation design by integrating the multi-zone model with CFD simulation,” PhD Thesis, Massachusetts Institute of Technology.

McDowell, T.P., Emmerich, S., Thornton, J.W., Walton, G., 2003. “Integration of Airflow and Energy Simulation Using CONTAM and TRNSYS”, ASHRAE Transactions, Vol. 109, No. 1.

Mehta, M., 2005. “Natural Ventilation Analyses of an Office Building with Open Atrium”, Ninth International IBPSA Conference, 2005.

Walker, C., S. Manchanda, H. Spindler and L. Norford, 2004. “Building Performance: Analysis of Naturally Ventilated UK Office Building,” RoomVent 2004, Coimbra.

NOMENCLATURE

ρ - Density of the air in $kg \cdot m^{-3}$	γ_s - absorptance of the surface for solar radiation (assumed the same value for the ceiling and the floor)
V - Volume of the space in m^{-3}	γ_i - absorptance of the surface for infrared radiation (assumed the same value for the ceiling and the floor)
c_p - Specific heat of air in $J \cdot kg^{-1} \cdot K^{-1}$	S_{sol} – solar radiation coming from windows in W
T_i - Temperature of zone i in ºC	S_{equ} – solar radiation coming from windows in W
t - Time in s	S_{occ} – solar radiation coming from windows in W
f_{ij} - Mass flowrate from zone i to j in kg/s	X_{fc} – view factor from the floor to ceiling
S_i - Heat source strength in zone i in W	T_c – Ceiling surface temperature in ºC
h - Convective heat transfer coefficient between air and thermal mass in $W \cdot m^{-2} \cdot K^{-1}$	T_f – Floor surface temperature in ºC
A - Contact area of the thermal mass in m^2	h_r – effective thermal resistant between the ceiling and the floor surfaces (through radiation) in $W \cdot m^{-2} \cdot K^{-1}$
T_{m1} - Temperature of the first thermal mass layer in ºC	x – thickness of the first layer of thermal mass in m
L - Thickness of a slab in m	Q_c – radiative solar and internal heat grain transferred to the ceiling surface in W
k - Thermal conductivity of the thermal mass in $W \cdot m^{-1} \cdot K^{-1}$	Q_f – radiative solar and internal heat gain transferred to the floor surface in W
Q_{b1}, Q_{b2} - direct absorption of the thermal mass in W	
α - The portion of the heat sources that were absorbed by the thermal mass	